Multifunctional halloysite and hectorite catalysts for effective transformation of biomass to biodiesel

Michele Casiello[1], Stefano Savino[1], Marina Massaro[2], Leonarda Francesca Liotta [3], Giuseppe Nicotra[4], Carlo Pastore[5], Caterina Fusco[6], Antonio Monopoli[1,6], Lucia D'Accolti[1,6,*], Angelo Nacci[1,6] and Serena Riela[2,*]

[1]Dipartimento di Chimica, Università di Bari "Aldo Moro", via Orabona 4, 70125 Bari, Italy. E-mail: lucia.daccolti@uniba.it
[2]Dipartimento STEBICEF, Sez. Chimica, Università degli Studi di Palermo, Viale delle Scienze, Ed. 17 "Stanislao Cannizzaro", 90128 Palermo, Italy. E-mail: serena.riela@unipa.it
[3]CNR-ISMN, Via Ugo La Malfa 153, Palermo, 90146, Italy.
[4]CNR-IMM, Zona Industriale Strada VIII, 5, Catania 95121, Italy.
[5]CNR-IRSA, via De Blasio 5, 70132 Bari, Italy.
[6]ICCOM-CNR, SS Bari, Via Orabona 4, 70126 Bari, Italy

Abstract: Halloysite surface was modified with tetrabutylammonium iodide, and then the obtained nanomaterial was used as support for ZnO nanoparticles. After characterization, the nanomaterial was used as a catalyst for fatty acid methyl esters (FAMEs) production. The recyclability of the nanomaterial was also investigated, and the optimization of reaction conditions by the design of experiments approach was performed as well. In addition, the synthesized nanomaterial was tested as a catalyst for FAME production from a series of waste lipids affording biodiesel in moderate to good yields (35-95%), depending on the matrix. To fully exploit the feasibility of clay minerals as catalysts in biodiesel formation, a screening of different clay minerals with different morphologies and compositions, such as sepiolite, palygorskite, bentonite, and hectorite was also performed in the esterification of FFAs (a mixture of 1:1 palmitic and stearic acids). Finally, hectorite, chosen as a model of 2:1 clay minerals, was covalently modified, and tested as a catalyst in the esterification of FFAs.

Keywords: clay minerals; heterogeneous catalysis; fatty acid methyl esters; waste lipids; ZnO nanoparticles.

1. Introduction

The global climate crisis, the problems related to the depletion of natural resources, and the gradual transition from the linear to the circular economic model are increasingly pushing the scientific community towards the valorization of wastes and their reintegration into the production cycle (Wang et al., 2022).

In this context, particular attention has been focused on the utilization of waste biomass for making energy, in particular, to produce biofuels, a process representing an economic and sustainable way for reducing the dependency on fossil fuels and minimizing the greenhouse effect (Notarnicola et al., 2023). Among the biofuels, fatty acid methyl esters (FAMEs), namely biodiesel, are ideal and readily usable substitutes for petro-diesel since they can be utilized without any engine modification. The employment of FAMEs in thermic engines can exert beneficial effects by reducing the emissions of particulate matter, dangerous aromatic compounds, and sulfur derivatives into the environment. Usually, FAMEs are produced *via* acid- or base-catalyzed transesterification of triglycerides and esterification of free fatty acids. The use of functional materials with high catalytic performances is crucial in industrial processes because it allows the replacement of polluting homogeneous catalysts with recyclable and eco-compatible heterogeneous catalysts. The catalytic activity is due to the presence of active sites on the surface structure of the materials, and according to their nature, they can be classified as acids or bases.

In this context, clay minerals (Zhou and Keeling, 2013), a class of natural inorganic layered compounds, with their high specific surface area, high mechanical and thermal stability, and, in some cases, ion-exchange capacity, which can be engineered into various functional heterogeneous catalysts, have recently attracted attention (Alves et al., 2014; Murray, 2006; Naeem et al., 2022; Nagendrappa and Chowreddy, 2021; Silva et al., 2014). Each clay mineral is constituted of 1:1 or 2:1 layers, containing, one or two silica tetrahedral sheets, respectively, joined to a central alumina, or other metal ions, octahedral sheet by sharing the apical oxygen atoms of the silica.

Clay minerals are very abundant on the earth, and their use in industry is widespread with numerous applications (Boulahbal et al., 2022; Cecilia and Jiménez-Gómez, 2021).

Clay minerals involved in the effective transformation of biomass into biodiesel are halloysite (Hal, Si/Al 1:1) (Pandey et al., 2020), hectorite (Ht, Si/Mg 2:1) (Zhang et al., 2019), sepiolite (Sep, Si/Mg 2:1) (Aslan et al., 2019; Degirmenbasi et al., 2014), and palygorskite (Pal, Si/Mg 2:1) (Li and Jiang, 2018; Zhang et al., 2017) and some clays for example bentonite (Bent, Si/Al 2:1) (da Costa and de

Andrade Lima, 2021; Ulakpa et al., 2022) (Figure 1). In addition, the design and synthesis of novel nanomaterials based on clay minerals and metal nanoparticles open up the possibility of their use for applications in green and sustainable catalysis (Glotov et al., 2021; Massaro et al., 2018; Massaro et al., 2019; Stavitskaya et al., 2022; Stavitskaya et al., 2020).

The use of halloysite, a clay mineral of the kaolin group, as support for nanoparticles has been very useful in obtaining catalysts that have shown enhanced catalytic performances (Massaro et al., 2022a). For example, Hal was successfully used by us as support in the ZnO nanoparticle-catalyzed transesterification of triglycerides (Massaro et al., 2020). From this study, clearly emerged a strong synergistic effect between ZnO supported onto Hal and tetraalkylammonium-based ionic liquids, that were used as additives playing the role of phase transfer catalysts (PTC) (Casiello et al., 2019; Casiello et al., 2021). Although efficient, the as-composed, semi-heterogeneous catalytic system showed the drawback of long and tedious separation and recycling procedures.

The esterification reaction of free fatty acids (FFAs) is an alternative method to the transesterification of triglycerides because it permits the use of fat wastes and byproducts such as olive oil wastewater, solid extract of municipal sewage scum, and so on. In addition, the FFAs, as raw materials, are very cheap compared to soybean oil, so they are a good alternative for biodiesel production. The acid activation of the Bent was proven to increase the catalytic performance with high stability and reusability compared to the commercial Amberlyst 15 catalyst (Jeenpadiphat and Tungasmita, 2013). Recently, Freire, Peixoto, *et al.* reported an organosulfonic-modified montmorillonite (Mt) as in the esterification of hybrid feedstocks, a mixture of FFA with different degrees of unsaturation and different carbon chain lengths obtaining promising performance (Silva et al., 2020). The same authors also reported the modification of Hal with an organosilane bearing thiol terminal groups that, after oxidation, allowed them to obtain sulfonic groups on the Hal surface as catalysts for the esterification reaction of a mixture of saturated and unsaturated FFAs (Silva et al., 2018).

The main objective of the present study was to modify clay mineral surfaces with both PCT and ZnO nanoparticles to obtain new heterogeneous catalysts, fully recyclable, and to evaluate their catalytic performances for biodiesel production.

Firstly, the Hal surface was modified with a PCT such as tetrabutylammonium iodide, and then the obtained nanomaterial was used as support for ZnO nanoparticles (Hal-TBAI@ZnO). After characterization, the nanomaterial was used as a catalyst for FAMEs production, first to investigate the transesterification of soybean oil and then, the esterification reaction of FFAs by means of methanol. The recyclability of the nanomaterial was also investigated, and the optimization of reaction conditions by the design of experiments (DoE) approach was performed as well. In addition, the synthesized nanomaterial was tested on real matrixes derived from a series of waste lipids. To fully exploit the feasibility of clay minerals as catalysts in biodiesel production, a screening of different clay minerals with different morphologies was also performed in the esterification of FFAs (a mixture of 1:1 palmitic and stearic acids) (Figure 1). The different catalytic activities were explained in terms of the acid/base properties and morphologies of the clays. Furthermore, to extend the modification strategy above described to a 2:1 clay mineral, Ht, chosen as the model, was modified, and tested as a catalyst in the esterification of FFAs.

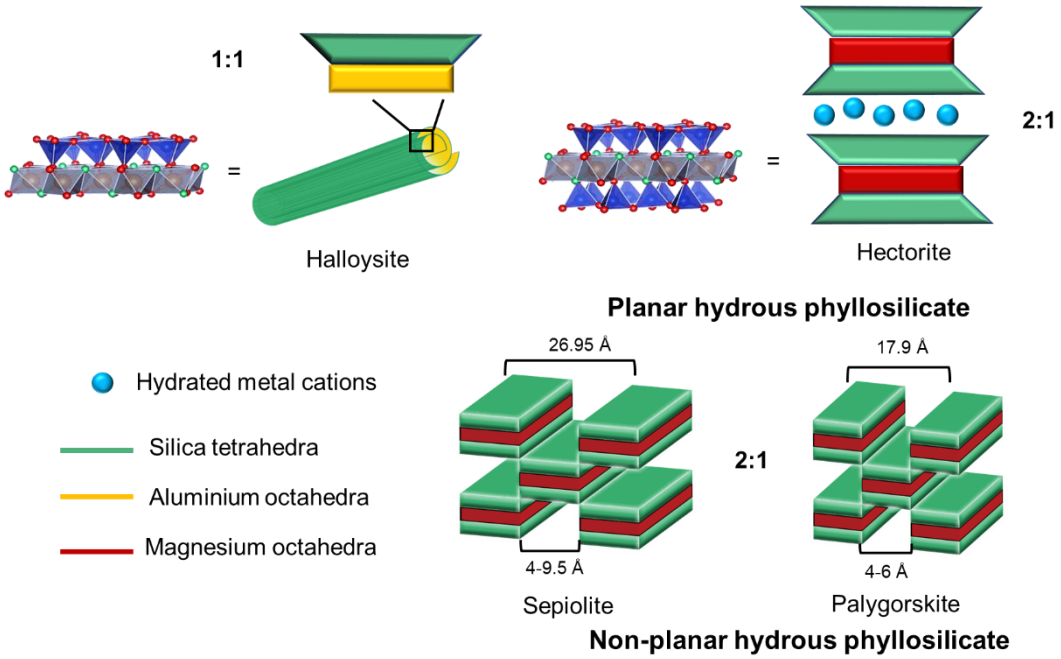

(a)

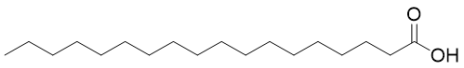

Stearic acid

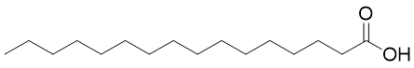

Palmitic acid

(b)

Figure 1. a) Structure of the clay minerals investigated for biodiesel production b) structure of FFAs used for esterification reaction.

2. Experimental

2.1 Materials

Chemicals (Palmitic Acid, Stearic Acid, n-Hexadecane) and solvents (methanol, ethyl acetate) were purchased from Sigma Aldrich. Halloysite was purchased from Merck, Ht, Sep, Pal, and Bent were kindly gifted by Tolsa Group Inc. (Madrid, Spain).

Commercial soybean oil was from Valsoia S.p.A. Bologna, Italy. The fatty acid composition consists of palmitic acid 10.35%, stearic acid 4.45%, oleic acid 22.60%, linoleic acid 30.95%, linolenic acid 6.84%, cis-11-eicosanoic acid 3.1%, behenic acid 0.36%, arachidic acid 0.36%, others 1%.

Waste cooking oil was a domestic source and olein residue was furnished by an Apulian oil company. Municipal sewage scum was sampled from the municipal wastewater treatment plant of Polignano (Bari, Italy). Fish oil, a gift from Greenswitch Biorefinery (Ferrandina, Italy), was used as received.

2.2. Syntheses

2.2.1 Synthesis of Hal-NH_2 and Ht-NH_2 nanomaterials

The Hal-NH_2 nanomaterial was synthetized by reacting 1 g of Hal in the presence of 2 mL of 3-aminopropyltrimethoxysilane in dry toluene (60 mL) under stirring and reflux conditions for 24 h. Afterwards, the crude solid was filtered off, washed with several aliquots of MeOH, and dried overnight at 80°C under a vacuum.

For Ht-NH_2 nanomaterial synthesis, 1 g of Ht was weighed in a microwave (MW) test tube provided with a cap, and 2 mL of 3-aminopropyltrimethoxysilane was added dropwise. The mixture was dispersed by ultrasound for 30 min at room temperature and inserted in an MW apparatus at 100°C under constant stirring for 1 h. The powder was filtered, rinsed with MeOH and dried at 80°C under vacuum.

2.2.2 Synthesis of Hal-TBAI@ZnO and Ht-TBAI@ZnO catalysts

To a dispersion of Hal-NH_2 or Ht-NH_2 (1 g) in anhydrous toluene (15 mL), iodobutane (8 g, 0.04 mmol), and pyridine (0.5 mL) were added. The obtained mixture was left to stir under reflux for 24 h. After this time the solvent was removed by filtration, the powder was rinsed several times with water and dichloromethane and finally dried at 60°C overnight to give the final Hal@TBAI or Ht-TBAI nanomaterials.

Hal-TBAI@ZnO and Ht-TBAI@ZnO were prepared by mixing 1 g of commercially available ZnO nanoparticles and 1 g of Hal@TBAI or Ht-TBAI in 30 mL of phosphate buffer solution (0.01 M) at pH 8.0. The mixture was stirred for 24 h at room temperature. Afterwards, the dispersion was centrifuged, and the solid precipitate was washed several times with deionized water (ca. 200 mL).

The white powders obtained were dried at 60°C overnight. The supernatant solution containing the unreacted ZnO was evaporated to recover ZnO.

2.3 Catalytic tests

Catalytic tests were carried out in 10 mL glass vials equipped with a magnetic bar and sealed with a screw cap.

In a typical experiment, clay-based nanomaterials (20 mg), lipid, (palmitic acid 150 mg, stearic acid 150 mg or soybean oil 326 μL=300 mg), and methanol (4 mL). The vial was then sealed, heated under stirring, and left to react for the proper time. After the reaction time, the mixture was cooled to room temperature, transferred into a centrifuge tube, and subjected to 4000 rpm for 10 min.

After centrifugation, the methanolic phase (containing FAMEs) was removed by means of a Pasteur pipette. Then the clay-based nanomaterials were washed with fresh methanol and centrifugated to eliminate traces of biodiesel. 100 μL of n-hexadecane was added to the methanolic phase as an internal standard, then the solution was evaporated to a small volume, and suspended in 10 mL of ethyl acetate. The ethyl acetate solution was subjected to qualitative and quantitative analyses by GC-MS to identify FAMEs and determine the composition of the biodiesel product (see SI).

2.4 Procedure for Catalyst Recycling

A series of five recycling experiments were carried out to assess the reusability of Hal-TBAI@ZnO nanomaterial under the optimized conditions established by the DOE method in sect. 2.4.1: FFAs (150 mg palmitic acid + 150 mg stearic acid), *T*= 95°C, cat. 25 mg, time 18 hours, MeOH 4 mL.

The typical procedure adopted in the five experiments was as follows: after completion of the reaction, the mixture was transferred into a centrifuge tube and subjected to 3500 rpm for 15 min. After centrifugation, the methanolic phase (containing FAMEs) was removed by means of a Pasteur pipette. Then, the Hal-TBAI@ZnO nanomaterial was washed with fresh methanol and centrifugated to eliminate traces of biodiesel. Collected methanolic phases were subjected to quantitative analyses for FAMEs yields by GC-MS, while Hal-TBAI@ZnO nanomaterial was washed again with ethyl

acetate to remove further traces of FAMEs and dried in an oven at 80°C for 2 hours. Then, it was weighed to evaluate its lost (1-2 mg ca. for each run). Then it was transferred in the glass vial reactor for a new run.

3. Results and discussion

3.1 Synthesis and characterization of Hal-TBAI@ZnO nanomaterials

Firstly, Hal external surface was modified by 3-amino trimethoxypropyl silane (Massaro et al., 2022b) by reaction of this with the few silanol groups present at the external surface as structural defects, affording the Hal-NH_2 nanomaterial which possesses a degree of functionalization, estimated by thermogravimetric analysis (TGA), of 0.4 mmol·g^{-1}. Afterward, the amino groups were subjected to quaternization with iodobutane obtaining the Hal-TBAI nanomaterial that showed a degree of functionalization of 0.3 mmol·g^{-1}. Based on the stoichiometric ratios between the amino groups on Hal external surface, and the final ammonium salts a mole ratio $-NH_2/-NR_3^+$ of 1:0.9 was achieved, indicating the successful modification. Finally, the Hal-TBAI nanomaterial was used as support for the immobilization of commercially available ZnO nanoparticles in phosphate buffer pH 8.0 at room temperature. In details, to a suspension of ZnO in phosphate buffer (10 mM) pH 8.0, Hal powder in a mass ratio 1:1 was added. As already reported, during the immobilization process, some Zn^{2+} ions were generated in alkaline conditions which could be linked to the siloxane groups present onto the clay by an O-Zn^{2+} coordination bond and some of them eventually could form covalent bonds with clays, rather than weak physical interactions (Massaro et al., 2020). Furthermore, due to the presence of positively charged functionalities onto Hal external surface, some ZnO nanoparticles could be formed inside Hal lumen because electrostatic repulsion between the -NR_3^+ groups and Zn^{2+} ions. After work-up the nanomaterial labeled as Hal-TBAI@ZnO (Figure 2) was obtained. The amount of ZnO immobilized onto the nanomaterial was estimated by ICP-OES and TGA as large as 30 wt%.

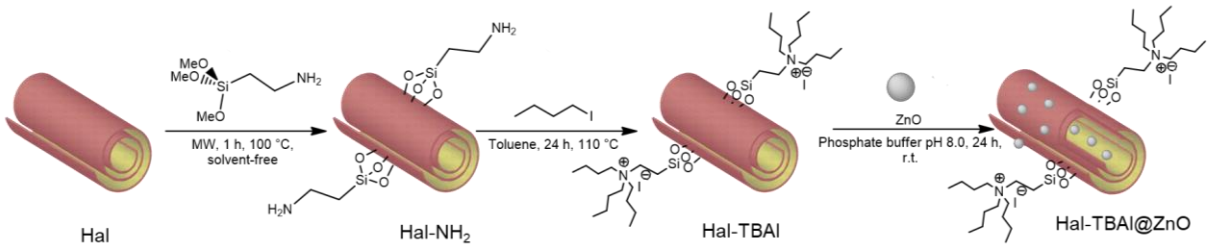

Figure 2. Schematic representation of the synthesis of Hal-TBAI@ZnO nanomaterial.

The successful modification was verified by FT-IR spectroscopy and TGA, and the catalyst morphology was imaged by Z-contrast Scanning Transmission Electron Microscopy (S/TEM).

In Figure 3a a comparison of the FT-IR spectra of Hal-NH_2, Hal-TBAI nanomaterials, and that of pristine Hal is reported. As it is possible to observe, in the FT-IR spectra of Hal-NH_2, besides the typical vibration bands of halloysite, new bands are present, in particular, the vibration bands for C–H stretching of methylene groups around 2980 cm^{-1} and the vibration band at ~1560 cm^{-1} due to the bending vibrations of the -NH_2 groups are observed. The latter bands disappeared after the quaternization reaction, further indicating the successful modification. In addition, the FT-IR spectra of Hal-TBAI showed a vibration band at ca. 1450 cm^{-1} attributable to the vibration band of the alkyl ammonium ions (in particular the vibration of the terminal -CH_3 group). After ZnO immobilization, it is possible to observe the presence of new signals in the range 500-470 cm^{-1} (Figure 3a), due to the stretching vibration of the ZnO group as already reported (Massaro et al., 2020).

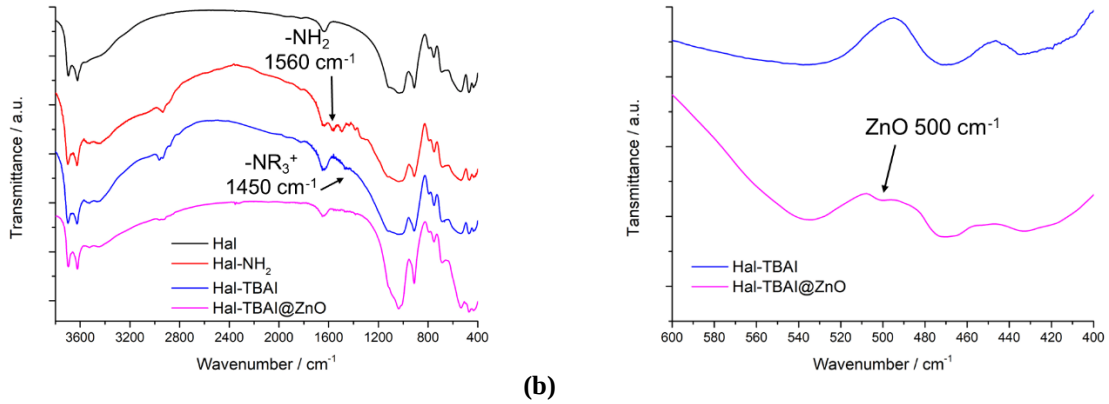

(a) **(b)**

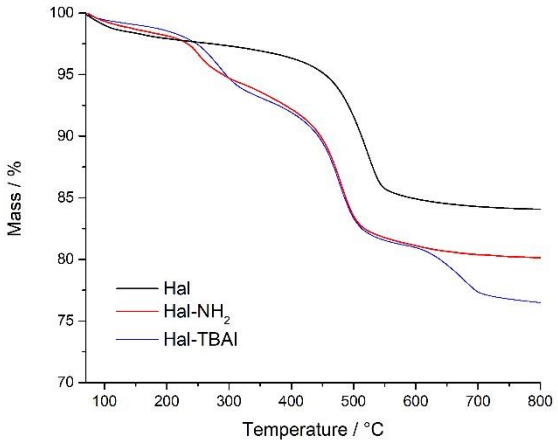

(c)

Figure 3. (a-b) FT-IR spectra and (c) thermogravimetric curves of Hal, Hal-NH_2, Hal-TBAI and Hal-TBAI@ZnO nanomaterials.

The thermal stability of the Hal-TBAI nanomaterial was investigated by TGA. As it is possible to note from Figure 3c, the Hal-NH_2 precursor showed the typical halloysite mass losses occurring at ca. 550°C, attributed to the removal of interlayer water molecules and the mass losses due to the thermal degradation of the organic moiety on Hal external surface (300 – 400°C). After the alkylation, a further mass loss above 500°C occurs, due to the oxidation of the organic moieties. A residual mass corresponding to 76.5 wt% was registered corresponding to the formation of a cationic salt. Based on the final mass value it was possible to calculate the percent loading discussed above.

Z-contrast Scanning Transmission Electron Microscopy (S/TEM) images showed that the morphology of the Hal-TBAI@ZnO nanomaterial was like that of pristine Hal. As it is possible to observe from Figure 4a-c, the nanomaterial shows a tubular hollow structure with rougher and less defined external surfaces in comparison to those of pristine halloysite, indicating that the modifications occurred (Figure 4A). Furthermore, the ZnO nanoparticles, clearly visible since their brighter intensity due to their higher atomic number Z, were also uniformly distributed inside the Hal lumen (Figure 4B). High-resolution HR-TEM micrographs of the ZnO nanoparticles supported on HNTs-TBAI nanomaterial (Figure 4C) showed crystallites with an average inter-fringe distance of 0.25 nm, which could be attributed to the (100) plane of the hexagonal wurtzite ZnO structure. From statistical analysis, the nanomaterial showed the presence of small ZnO nanoparticles with an average

diameter of 3.3 ± 0.7 nm and narrow size distribution (Figure 4D) smaller than that of ZnO bulk (Massaro et al., 2020).

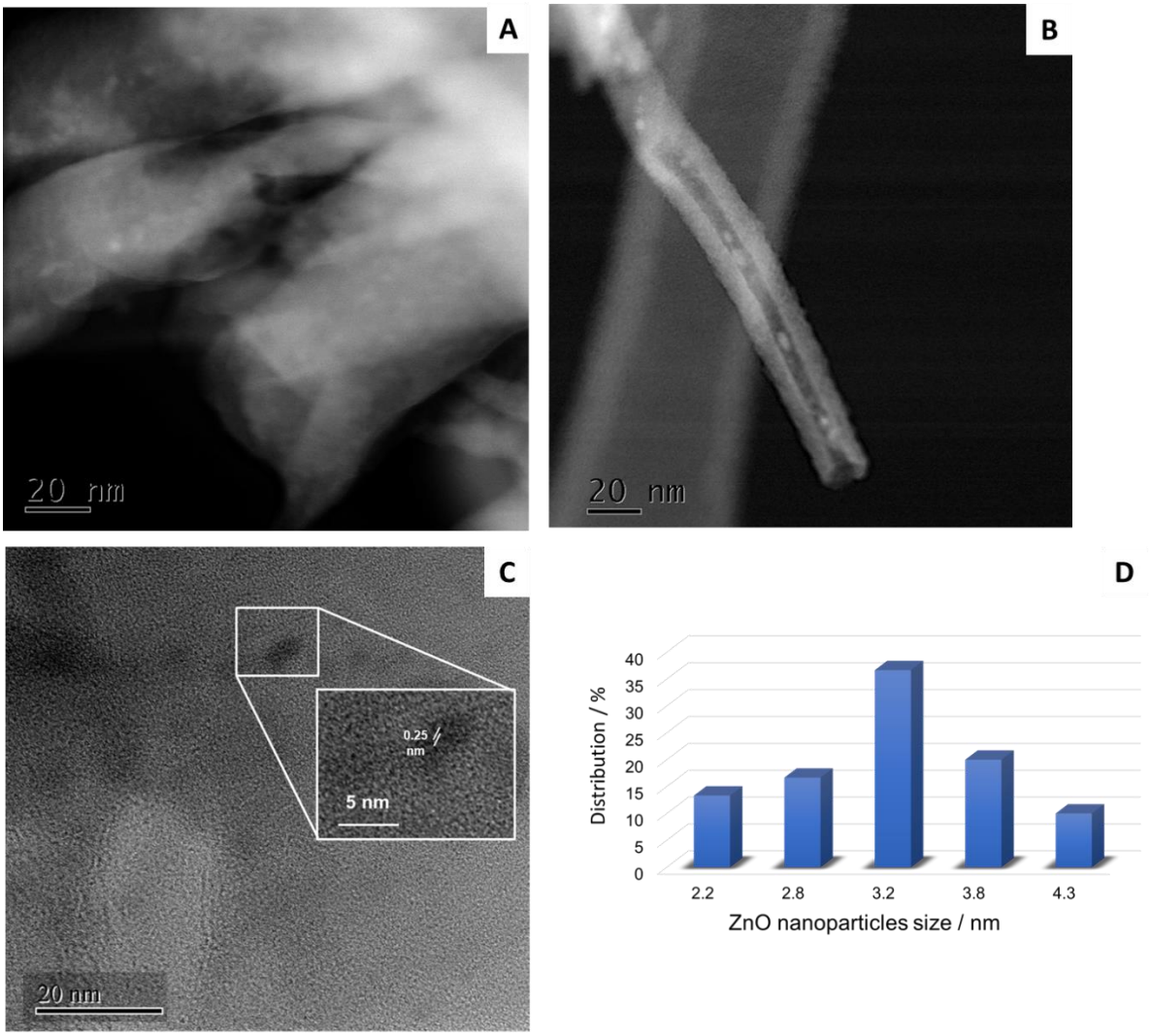

Figure 4. (A-B) Z-Contrast S/TEM images and (C) HR-TEM of HNTs-TBAI@ZnO nanomaterial; (D) ZnO nanoparticles distribution (n = 30).

3.2 Catalytic tests with Hal-TBAI@ZnO

The catalytic performances of the synthetized Hal-TBAI@ZnO nanomaterial were first investigated on the transesterification reaction of soybean oil under different experimental conditions. This reaction was chosen since our previous results (Massaro et al., 2020) with a Hal@ZnO catalyst in the presence of TBAI (0.33 mmol) showed that the modification could improve the Hal catalytic performance and the recyclability of ZnO nanoparticles (FAME yield 95%). The obtained results are

listed in Table 1. The screened ranges of temperatures (70–120°C) and times (7-24 h) were chosen to establish the limit values of DOE (*vide infra*).

Table 1. FAME production by the transesterification reaction of soybean oil in the presence of Hal-TBAI@ZnO catalyst.

Entry	Catalyst	Temperature (°C)	Time (h)	FAME Yield (%)[a]
1	Hal	70	7	<5
2	Hal-TBAI@ZnO[b]	70	7	<5
3	Hal-TBAI@ZnO[b]	110	7	24±2
4	Hal-TBAI@ZnO[b]	110	24	27±1
5	Hal	120	24	<5
6	Hal@ZnO[c]	120	24	10.5±0.2
7	Hal-TBAI@ZnO[b]	120	24	30±2

[a] Determined by GC-MS. [b] Amount of TBAI grafted on Hal-TBAI@ZnO catalyst 0.06 mmol; [c] amount of TBAI added in the presence of Hal@ZnO catalyst 0.06 mmol.

As it is possible to observe, the best experimental conditions were obtained at 120°C for a reaction time of 24 h (Entry 7). This agrees with literature data which report that the transesterification reaction is an endothermic process with a positive $\Delta H^{\#}$ value (Casiello et al., 2019). From the data reported in Table 1, it is also possible to note that an increase in the reaction time produces only a slight enhancement in the FAME yield, thus it is possible to hypothesize that the transesterification reaction could occur in a shorter time than 24 h. Although at first glance this value appears lower than the yield previously obtained with Hal@ZnO catalyst (Massaro et al., 2020), it should be noted that the amount of TBAI covalently linked on the Hal surface in Hal-TBAI@ZnO is ca. 20% (0.06 mmol) of that previously reported (Massaro et al., 2020). By carrying out the reaction with Hal@ZnO catalyst and adding the same amount of TBAI (0.06 mmol) present onto Hal-TBAI, a decrease in the FAMEs yield was observed (Entry 6), indicating that the fully heterogenized catalyst is advantageous for the reaction.

However, these results, albeit encouraging, showed that this kind of catalyst is not advantageous for the transesterification of soybean oil. This result could be explained by mechanistic considerations. In the transesterification reaction, ZnO, being amphoteric, acts as a bifunctional Lewis acid/base catalyst, capable of generating CH_3O^- anions (through the basic sites represented by oxygen atoms at the surface), but it is also able to activate the carboxyl group by means of acid sites represented by Zn atoms. In this process, the TBAI assumes the role of PTC by transferring methoxide anions into the oil phase. In our case, the amount of TBAI anchored onto the Hal surface is probably not enough to ensure the complete transfer and this decreases the catalytic performances. However, it should be noted that the confinement of TBAI units onto the Hal surface is advantageous since it increases the local concentration of the PCT increasing the FAMEs yield (entry 7).

Based on these results, a different kind of reaction was tested, in particular the esterification of a 1:1 mass ratio mixture of palmitic and stearic acids, as the FFAs model, which is a process that requires acidic conditions. Different temperatures were screened, and the obtained results are reported in Table 2. As it is possible to observe, from this preliminary screening the temperature is a crucial parameter to increase the FAME yield in the presence of Hal-TBAI@ZnO. The good results obtained could be explained both by the presence of the ZnO onto both surfaces of Hal-TBAI@ZnO nanomaterial as an acid site, and in the linear structure of FFA molecules. These, indeed, could be efficiently loaded inside the Hal lumen by hydrophobic effects, which act as a nanoreactor for the esterification reaction.

Table 2. FAME production by the esterification reaction of a mixture of palmitic and stearic acid 1:1 w:w in the presence of Hal-TBAI@ZnO catalyst.

Entry	Catalyst	Temperature (°C)	FAME Yield (%)[(a)]
1	Hal-TBAI@ZnO	90	8±1
2	Hal-TBAI@ZnO	100	55±1
3	Hal-TBAI@ZnO	110	65±2
4	Hal-TBAI@ZnO	120	99±1

5	Hal	120	54±2

[a] Determined by GC-MS.

It should be noted that both transesterification and esterification reactions did not occur without ZnO, while, as already reported, no satisfactory yields were obtained in the presence of either bulk ZnO or sole TBAI, while the physical mixture of the three components (Hal, ZnO_{bulk} and TBAI), although affords satisfactory yield, is not fully recyclable (Casiello et al., 2019; Massaro et al., 2020).

3.2.1 Optimization of reaction conditions: application of DOE Method

Based on the preliminary screening, it is clear that at least three parameters could affect biodiesel yields, namely catalyst mass, temperature, and reaction time. For this reason, an optimization of the reaction conditions was conducted with the DOE method approach.

To fully investigate the direct esterification of fatty acids with Hal-TBAI@ZnO, fifteen experiments were statistically required by Box-Behnken design (Table 3). Ranges similar to those established in the previous experiments were chosen for applying the DOE method, and specifically: catalyst mass (Hal-TBAI@ZnO) = 5 – 35 mg, T = 90 – 130°C, and time = 18 – 24 h.

Results of the experiments reported in Table 3 were analysed to assess the "goodness of fit" and details on the statistical elaboration (regression equation, interaction diagrams, model summary, etc.) are reported in the supporting information section.

The Pareto diagram (Figure 5a) highlights how the factors affecting the final yield are the temperature and the amount of Hal-TBAI@ZnO nanomaterial (mg). The time factor, within the interval explored, seemed to have only a slight effect. The main effects diagram (Figure 5b) shows that the Hal-TBAI@ZnO amount does not reach a plateau after 35 mg, although tests performed outside the design indicate that higher Hal-TBAI@ZnO amounts do not result in significant increments of yield (see supporting information).

Table 3. DOE experiments for the esterification of FFAs catalyzed by Hal-TBAI@ZnO.

Entry	Hal-TBAI@ZnO (mg)	Time (h)	Temperature (°C)	FAME Yield (%)
1	5	21	130	77.1
2	35	21	130	100.0
3	35	24	110	100.0
4	35	18	110	97.5
5	20	21	110	69.7
6	20	21	110	65.4
7	20	24	90	15.0
8	20	24	130	100.0
9	5	18	110	28.4
10	5	21	90	9.2
11	20	18	130	100.0
12	20	21	110	71.3
13	5	24	110	28.8
14	35	21	90	32.0
15	20	18	90	12.4

Results of the experiments elaborated using Minitab software, reported in Table 3 were analysed to assess the "goodness of fit" and details on the statistical elaboration such as model summary, regression equation, and interaction diagrams are reported in supporting information.

The Pareto diagram (Figure S.1) highlights how the factors affecting the final yield are the temperature (T) and the amount of Hal-TBAI@ZnO (mg). The time factor, within the interval explored, seemed to have only a slight effect. The main effects diagram (Figure S.2) shows that the Hal-TBAI@ZnO amount does not reach a plateau after 35 mg, although tests performed outside the design indicate that higher Hal-TBAI@ZnO amounts do not result in significant increments of yield (see SI).

This is better highlighted in the interaction plot diagram showing that the quantity of Hal-TBAI@ZnO affects the final yield up to 20 mg, while with 35 mg a plateau is reached at 110°C (see SI). The response surface graphs (Figure S.3) provide the optimal conditions to give 100% yield suggested by the statistical method that are: the amount of Hal-TBAI@ZnO 35 mg, time 21 h, temperature 116.542°C.

In the interaction plot diagram (Figure S.4) it is possible to observe how the various factors interact with each other. In the first box at the top left (enlarged in Figure S.5) it can be seen how the quantity of Hal-TBAI@ZnO affects the final yield up to 20 mg. At 35 mg a plateau is reached at 110°C.

The analysis of the response surface regression equation allowed to obtain the final solution of the method that shows the optimal reaction conditions as listed in Table 4.

Table 4. Solution of DOE method displaying the optimized conditions for the esterification of FFAs catalyzed by Hal-TBAI@ZnO.

Solution	Time	Temperature	Hal-TBAI@ZnO (mg)	Yields Fit	Nanomaterial Desirability
1	21	116.542	35	100.000	1.00000

3.2.2 Recycling experiments

Recycling experiments were also conducted to verify the recovery of the catalytic system Hal-TBAI@ZnO and assure that no residues are released into the biodiesel product during the work-up procedure. Recycling experiments showed that after being reused 5 times, Hal-TBAI@ZnO nanomaterial proved to be stable enough, as the biodiesel yields decreased slowly from 99% to 77% (Figure 6). The slight decrease in activity could be due to small losses of catalytic material during manipulations or to absorption phenomena of both lipid feedstocks and FAMEs products inside the Hal lumen that could inhibit the catalytic process. The absence of leaching of ZnO into the reaction mixture was ascertained by ICP-OES. A similar trend of operational stability had been previously observed for the analogous catalyst HNT@ZnO catalyst devoid of tetraalkylammonium functionalities on the surface (Massaro et al., 2020).

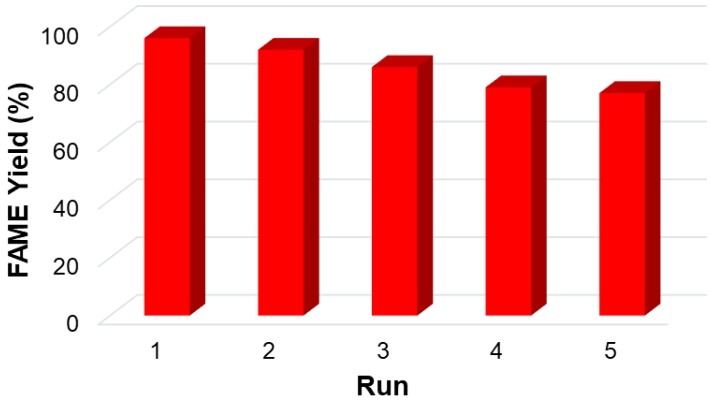

Figure 6. Recycling test of Hal-TBAI@ZnO nanomaterial in the conversion of the model mixture of FFAs into FAMEs.

3.2.3 Literature comparison

The catalytic performances of Hal-TBAI@ZnO nanomaterial were compared with other reported heterogeneous catalysts used for the esterification of free fatty acids. As reported in Table 5, the synthetized catalyst showed good catalytic activity and recyclability than the other reported ones possessing the advantage to be constituted by bio- and eco-compatible, low-cost, and available in large amounts nanomaterials such as halloysite and ZnO nanoparticles.

Table 5. Comparison with other reported heterogeneous catalysts.

Catalyst	Feedstock	Temperature (°C)	FAME Yield and recyclability	Ref.
ZrO_2/SiO_2	Stearic acid	120	76.9% to 72.5% after 5 cycles	(Mahmoud et al., 2020)
$Ag_1(NH_4)_2PW_{12}O_{40}/UIO\text{-}_{66}$	Lauric acid	240	75% to 58% after 6 cycles	(Zhang et al., 2020)
Montmorillonite-based clay catalysts (KSF, KSF/0, KP10, and K10)	Stearic, oleic, and palmitic acids	150	97% to 84% after 3 cycles	(Bouguerra Neji et al., 2009)
PMA@Bi-BTC	Oleic acid	160	92.5% to 84.0% after 7 cycles	(Zhang et al., 2023)
$CrWMnO_2$	Palm fatty acid distillate	170	84% to 63% after 4 cycles	(Wan et al., 2017)
Hal-TBAI@ZnO	Palmitic and stearic acids mixture (1:1 w/w)	120	99% to 77% after 5 cycles	This work

3.2.4. Catalytic tests on waste lipids

Once optimized the experimental conditions, Hal-TBAI@ZnO nanomaterial was tested as a catalyst for FAMEs production from a series of waste lipids (Table 6). The protocol was applied to refined

and unrefined feedstocks coming from waste fats. Among them, WCO, lipid residues coming from the industrial processing of animal fats (fish oil), or olive oil, and even the lipid component of municipal sewage scum, were investigated as representative examples. Lipid composition of the feedstocks such as the transesterifiable/esterifiable amount was ascertained either by standard analyses or furnished by the supplier. As expected, modified Hal-TBAI@ZnO proved to be more efficient in giving esterification of lipids containing significant amounts of free fatty acids (Table 4, entries 1-3), thus confirming that this kind of catalyst is less suitable in the transesterification reactions that occur in lipid matrixes possessing mainly a triglycerides (Table 4, entries 4-6).

Table 6. Catalytic tests on waste lipids.

Entry	**Lipid matrix[b]**	**Yields (%)[c]**	**FFAs (wt %)**	**transester/ esterif am.nt (wt %)**
1	Solid extract of municipal sewage scum[d]	58	32	60
2	Olein residue (solid)[e]	95	76	96
3	Olive oil wastewater[e] (liquid)	61	75	62
4	Jatropha oil	42	<1	90
5	Fish oil	35	<1	96
6	Waste cooking oil (WCO)	30	2	96

[a] General reaction conditions: feedstock 300 mg and methanol 4 mL, catalyst 35 mg, T = 115°C, time 20-22 h. [b] The properties and composition of these lipid sources are given in SI. [c] GC-MS yields evaluated based on esterifiable/transesterifiable fraction of feedstock. [d] The lipid fraction of municipal sewage scum. [e] A highly acidic mixture of lipids coming from oil industry processing.

3.3 Esterification of FFAs in the presence of different clay minerals

To expand the use of the clay minerals, such as those of 2:1 stoichiometry, as catalysts for FAME production, the methanolic esterification of the 1:1 mixture of stearic and palmitic acid was

investigated in the presence of Pal, Sep, and Ht and of the Bent clay at two different temperatures and reaction times. The obtained results are reported in Figure 7 with those of Hal for comparison. As it is possible to observe, all clays investigated showed moderate catalytic performances with a FAME yield ranging from 25 to 50 wt% at 120°C for a reaction time of 24 h. The worst catalytic performances were observed in the case of Ht; whilst other clays follow the order Hal > Sep > Bent > Pal > Ht.

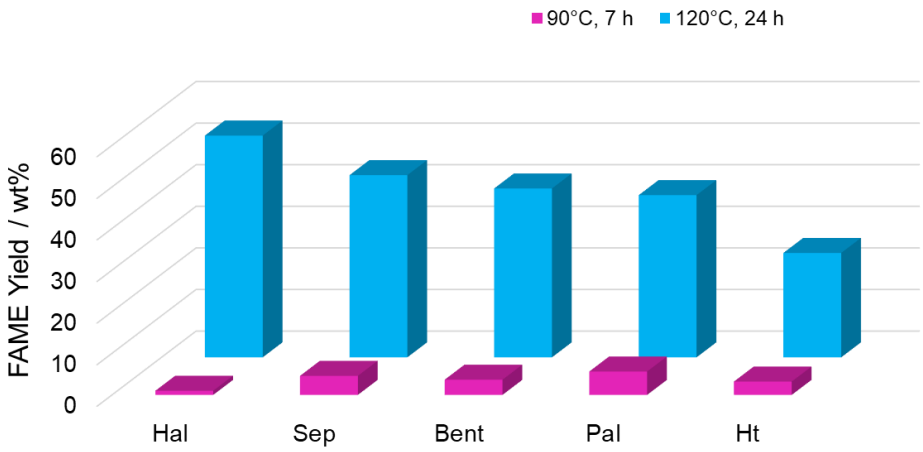

Figure 7. Catalytic performances of Hal, Sep, Pal, Bent, and Ht in the methanolic esterification of FFAs (1:1 mixture palmitic and stearic acid) at two different temperatures and reaction time.

Since the esterification reaction of FFAs is an acid-catalyzed process, the different results were explained considering the acid/base properties of the pristine nanomaterials investigated. It is indeed known that the basicity of clays and clay minerals is strictly influenced by their chemical composition and alkali oxide contents (Silva et al., 2014). In Table 7 are reported the chemical composition of the different clay minerals. As it is possible to note, Ht presents the largest amount of alkali oxides and thus, among the different clays is the one which possesses the highest basicity as also proved by the pH of an aqueous dispersion of it.

Table 7. Chemical composition and pH of the aqueous dispersion of the clay and clay minerals investigated.

Entry	SiO_2	Al_2O_3	MgO	CaO	Na_2O	K_2O	pH
Sepiolite (García-Villén et al., 2020)	59.58	3.44	22.44	5.27	0.17	0.36	8.5
Palygorskite (García-Villén et al., 2020)	59.65	3.43	22.43	0.56	0.14	0.95	9.5

Hectorite (García-Villén et al., 2021)	53.19	8.39	13.38	3.00	5.60	2.83	10.8
Halloysite	44.70	37.60	/	0.19	0.15	/	7.5
Bentonite (Viseras et al., 2000)	53.78	20.09	4.69	1.79	0.69	0.52	10.2

373

374 *3.3.2 Modification of Ht*

375 As described above, the modification of the clay mineral surface is a useful strategy to improve its
376 catalytic properties, thus, Ht was covalently modified, because of it showed the worst catalytic
377 performance in the esterification reaction (Figure 7). Conversely to Hal, Ht was modified at the edges,
378 where the silanol groups are mainly present (Colletti et al., 2020; Massaro et al., 2021; Notarbartolo
379 et al., 2022). modified hectorite (Ht-NH_2) possessing a degree of functionalization of 1 mmol g^{-1} was
380 subjected to quaternization with iodobutane affording the Ht-TBAI nanomaterial that showed a
381 degree of functionalization of 0.9 mmol·g^{-1} as estimated by TGA. Afterwards, ZnO nanoparticles
382 were immobilized on the support to give the final catalyst Ht-TBAI@ZnO with a ZnO loading percent
383 of 25 wt%.

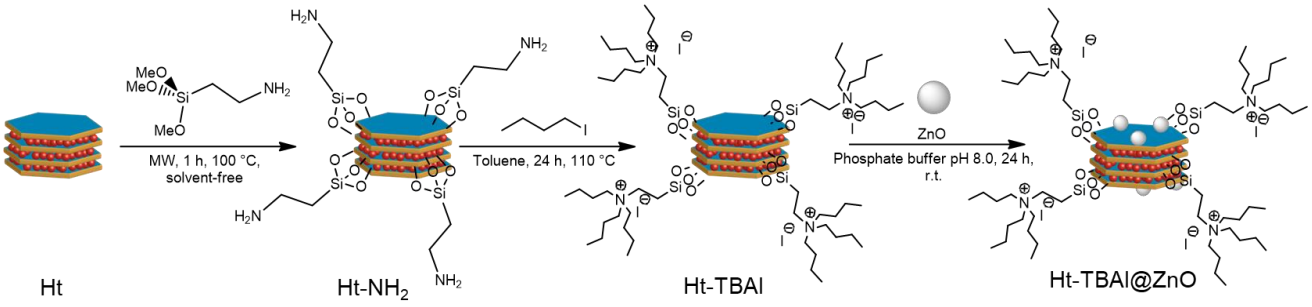

384

385 **Figure 8.** Schematic representation of the synthesis of Ht-TBAI@ZnO nanomaterial.

386 The successful modification of Ht was proved by FT-IR spectroscopy, TGA, and TEM investigations
387 (see SI) from which it was possible to draw the same consideration made for the Hal-TBAI@ZnO
388 nanomaterial.

389 *3.3.1 Catalytic activity of Ht-TBAI@ZnO nanomaterial*

The Ht-TBAI@ZnO nanomaterial was thus tested as a catalyst in the esterification reaction between methanol and FFAs at different temperatures and the obtained results are reported in Table 8. From the experimental data obtained, it is possible to conclude that the modification of Ht, by the introduction both of TBAI, directly linked at the Ht edges, and of the ZnO nanoparticles, enhances the catalytic properties of the nanomaterial in comparison to Ht at each temperature investigated. The increase in the catalytic activity compared to the pristine clay mineral was attributable to the presence of ZnO and TBAI on the Ht surface which acts both as an acid site and PTC.

Table 8. FAME production by the esterification reaction of FFAs in the presence of Ht-TBAI@ZnO nanomaterial.

Run	Catalyst	T (°C)	Time (h)	FAMEs Yield (%)[(a)]
1	Ht-TBAI@ZnO	90	24	42
2	Ht-TBAI@ZnO	100	24	63
3	Ht-TBAI@ZnO	110	24	77
4	Ht-TBAI@ZnO	120	24	86

[(a)] Determined by GC-MS

4. Conclusions

In conclusion, in this work covalently modified halloysite (Hal-TBAI@ZnO) was used as a catalyst in the transesterification/esterification of waste lipids for biodiesel production. First, the halloysite surface was modified with tetrabutylammonium iodide units to directly link a phase transfer catalyst onto the clay surface and then this nanomaterial was used as support for ZnO nanoparticles. The nanomaterial was thoroughly characterized by FT-IR spectroscopy and HAADF/STEM investigation, while the thermal stability was assessed by thermogravimetric analysis. Catalytic tests showed that the Hal-TBAI@ZnO nanomaterial has good activity in the esterification of free fatty acids, that are abundant in waste lipids coming from wastewater treatment (e.g. lipids extract from wastewater sludge, oil mill residue, etc.). The full heterogenization of the catalytic system allowed the synthesis of an efficient and recyclable catalyst made from a natural, low-cost, and abundant material such as halloysite. This could allow the scale-up of both the synthesis of the catalyst and the catalytic reactions for future industrial applications. In addition, it is noteworthy to mention that due to the bio-

end eco-compatibility of halloysite, once the catalyst is exhausted it could be used as raw material for other kinds of application.

Three different parameters were screened with the statistical DOE method, namely temperature, catalyst mass, and reaction time that gave the following best conditions to achieve the maximum yields: T = 116°C, Cat. 35 mg, time 21 h.

Furthermore, different clay minerals with different compositions and morphologies were investigated as catalysts in the esterification reaction of FFAs obtaining different results depending on their composition. Finally, to expand the application of the fully heterogenized catalyst, Ht, chosen as a model of 2:1 clay mineral was modified with TBAI units and used as support for ZnO nanoparticles. Catalytic tests on the esterification reaction showed once again the advantage of modification for the catalytic properties of the clay in comparison to the pristine one.

Author Contributions: "Conceptualization: S.R., L.D., A.N., methodology, M.C., S.S., M.M., L.F.L., G.N., C.P., C.F., A.M., L.D., A.N., S.R.; data curation, M.C., S.S., M.M., L.F.L., G.N., C.P., C.F., A.M., L.D., A.N., S.R.; writing—original draft preparation, L.D., A.N. and S.R.; writing—review and editing, L.D., M.M. and S.R., supervision, L.D., A.N., S.R."

Funding: "This research was partially funded by the European Union-19 FESR "PON Ricerca e Innovazione 2014–2020. Progetto: 20 Energie per l'Ambiente TARANTO-Cod. ARS01_00637" and by "Research for Innovation (REFIN)" – POR Puglia FESR FSE 2014-2020, Project ID 4A20B1C8.

Acknowledgment: The authors are grateful to Dr. Emma Lambert.

References

Alves, H.J., da Rocha, A.M., Monteiro, M.R., Moretti, C., Cabrelon, M.D., Schwengber, C.A., Milinsk, M.C., 2014. Treatment of clay with KF: New solid catalyst for biodiesel production. Appl. Clay Sci. 91-92, 98-104.

Aslan, S., Aka, N., Karaoglu, M.H., 2019. NaOH impregnated sepiolite based heterogeneous catalyst and its utilization for the production of biodiesel from canola oil. Energy Sources, Part A: Recovery, Utilization, and Environmental Effects 41, 290-297.

Bouguerra Neji, S., Trabelsi, M., Frikha, M.H., 2009. Esterification of Fatty Acids with Short-Chain Alcohols over Commercial Acid Clays in a Semi-Continuous Reactor. Energies 2, 1107-1117.

Boulahbal, M., Malouki, M.A., Canle, M., Redouane-Salah, Z., Devanesan, S., AlSalhi, M.S., Berkani, M., 2022. Removal of the industrial azo dye crystal violet using a natural clay: Characterization, kinetic modeling, and RSM optimization. Chemosphere 306, 135516.
Casiello, M., Catucci, L., Fracassi, F., Fusco, C., Laurenza, A.G., Di Bitonto, L., Pastore, C., D'Accolti, L., Nacci, A., 2019. ZnO/Ionic Liquid Catalyzed Biodiesel Production from Renewable and Waste Lipids as Feedstocks. Catalysts 9, 71.
Casiello, M., Losito, O., Aloia, A., Caputo, D., Fusco, C., Attrotto, R., Monopoli, A., Nacci, A., D'Accolti, L., 2021. Steel Slag as New Catalyst for the Synthesis of Fames from Soybean Oil. Catalysts 11, 619.
Cecilia, J.A., Jiménez-Gómez, C.P., 2021. Catalytic Applications of Clay Minerals and Hydrotalcites. Catalysts 11, 68.
Colletti, C.G., Massaro, M., Lazzara, G., Cavallaro, G., Milioto, S., Pibiri, I., Noto, R., Riela, S., 2020. Synthesis, characterization and study of covalently modified triazole LAPONITE® edges. Appl. Clay Sci. 187.
da Costa, J.M., de Andrade Lima, L.R.P., 2021. Transesterification of cotton oil with ethanol for biodiesel using a KF/bentonite solid catalyst. Fuel 293, 120446.
Degirmenbasi, N., Boz, N., Kalyon, D.M., 2014. Biofuel production via transesterification using sepiolite-supported alkaline catalysts. Appl. Catal. B 150-151, 147-156.
García-Villén, F., Sánchez-Espejo, R., Borrego-Sánchez, A., Cerezo, P., Sandri, G., Viseras, C., 2021. Assessment of Hectorite/Spring Water Hydrogels as Wound Healing Products. Proceedings 78, 6.
García-Villén, F., Sánchez-Espejo, R., López-Galindo, A., Cerezo, P., Viseras, C., 2020. Design and characterization of spring water hydrogels with natural inorganic excipients. Appl. Clay Sci. 197, 105772.
Glotov, A., Novikov, A., Stavitskaya, A., Nedolivko, V., Kopitsyn, D., Kuchierskaya, A., Ivanov, E., Stytsenko, V., Vinokurov, V., Lvov, Y., 2021. Nanoreactors based on hydrophobized tubular aluminosilicates decorated with ruthenium: Highly active and stable catalysts for aromatics hydrogenation. Catal. Today 378, 33-42.
Jeenpadiphat, S., Tungasmita, D.N., 2013. Acid-activated pillar bentonite as a novel catalyst for the esterification of high FFA oil. Powder Technol. 237, 634-640.
Li, Y., Jiang, Y., 2018. Preparation of a palygorskite supported KF/CaO catalyst and its application for biodiesel production via transesterification. RSC Adv. 8, 16013-16018.
Mahmoud, H.R., El-Molla, S.A., Ibrahim, M.M., 2020. Biodiesel production via stearic acid esterification over mesoporous ZrO2/SiO2 catalysts synthesized by surfactant-assisted sol-gel auto-combustion route. Renew. Energ. 160, 42-51.
Massaro, M., Casiello, M., D'Accolti, L., Lazzara, G., Nacci, A., Nicotra, G., Noto, R., Pettignano, A., Spinella, C., Riela, S., 2020. One-pot synthesis of ZnO nanoparticles supported on halloysite nanotubes for catalytic applications. Appl. Clay Sci. 189.
Massaro, M., Colletti, C.G., Buscemi, G., Cataldo, S., Guernelli, S., Lazzara, G., Liotta, L.F., Parisi, F., Pettignano, A., Riela, S., 2018. Palladium nanoparticles immobilized on halloysite nanotubes covered by a multilayer network for catalytic applications. New J. Chem. 42, 13938-13947.
Massaro, M., Colletti, C.G., Fiore, B., La Parola, V., Lazzara, G., Guernelli, S., Zaccheroni, N., Riela, S., 2019. Gold nanoparticles stabilized by modified halloysite nanotubes for catalytic applications. Appl. Organomet. Chem. 33, e4665.
Massaro, M., Iborra, C.V., Cavallaro, G., Colletti, C.G., García-villén, F., Lazzara, G., Riela, S., 2021. Synthesis and characterization of nanomaterial based on halloysite and hectorite clay minerals covalently bridged. Nanomaterials 11, 1-13.
Massaro, M., Noto, R., Riela, S., 2022a. Halloysite Nanotubes: Smart Nanomaterials in Catalysis. Catalysts 12, 149.
Massaro, M., Poma, P., Cavallaro, G., García-Villén, F., Lazzara, G., Notarbartolo, M., Muratore, N., Sánchez-Espejo, R., Viseras Iborra, C., Riela, S., 2022b. Prodrug based on halloysite delivery systems to improve the antitumor ability of methotrexate in leukemia cell lines. Colloids Surf. B 213.
Murray, H.H., 2006. Chapter 2 Structure and Composition of the Clay Minerals and their Physical and Chemical Properties, in: Murray, H.H. (Ed.), Developments in Clay Science. Elsevier, pp. 7-31.
Naeem, A., Zaman, S., Farooq, M., Khan, I.W., Ghazi, Z.A., Saeed, T., Hamayun, M., 2022. Biodiesel production from waste cooking oil employing natural bentonite supported heterogeneous catalyst: Waste to biodiesel. Korean J. Chem. Eng. 39, 1450-1459.

493 Nagendrappa, G., Chowreddy, R.R., 2021. Organic Reactions Using Clay and Clay-Supported Catalysts: A
494 Survey of Recent Literature. Catalysis Surveys from Asia 25, 231-278.
495 Notarbartolo, M., Massaro, M., de Melo Barbosa, R., Emili, C., Liotta, L.F., Poma, P., Raymo, F.M., Sànchez-
496 Espejo, R., Vago, R., Viseras-Iborra, C., Riela, S., 2022. Exploring the cellular uptake of hectorite clay mineral
497 and its drug carrier capabilities. Colloids Surf. B 220.
498 Notarnicola, B., Tassielli, G., Renzulli, P.A., Di Capua, R., Astuto, F., Riela, S., Nacci, A., Casiello, M., Testa, M.L.,
499 Liotta, L.F., Pastore, C., 2023. Life Cycle Assessment of a system for the extraction and transformation of
500 Waste Water Treatment Sludge (WWTS)-derived lipids into biodiesel. Sci. Total Environ. 883.
501 Pandey, G., Tharmavaram, M., Rawtani, D., 2020. Halloysite Nanotubes: An 'Aluminosilicate Nanosupport'
502 for Energy and Environmental Applications, in: Ledwani, L., Sangwai, J.S. (Eds.), Nanotechnology for Energy
503 and Environmental Engineering. Springer International Publishing, Cham, pp. 125-144.
504 Silva, L.C.A., Silva, E.A., Monteiro, M.R., Silva, C., Teleken, J.G., Alves, H.J., 2014. Effect of the chemical
505 composition of smectites used in KF/Clay catalysts on soybean oil transesterification into methyl esters. Appl.
506 Clay Sci. 102, 121-127.
507 Silva, S.M., Peixoto, A.F., Freire, C., 2018. HSO3-functionalized halloysite nanotubes: New acid catalysts for
508 esterification of free fatty acid mixture as hybrid feedstock model for biodiesel production. Appl. Catal. A
509 568, 221-230.
510 Silva, S.M., Peixoto, A.F., Freire, C., 2020. Organosulfonic acid functionalized montmorillonites as solid
511 catalysts for (trans) esterification of free fatty acids and (waste) oils. Renew. Energ. 146, 2416-2429.
512 Stavitskaya, A., Glotov, A., Pouresmaeil, F., Potapenko, K., Sitmukhanova, E., Mazurova, K., Ivanov, E.,
513 Kozlova, E., Vinokurov, V., Lvov, Y., 2022. CdS Quantum Dots in Hierarchical Mesoporous Silica Templated on
514 Clay Nanotubes: Implications for Photocatalytic Hydrogen Production. ACS Appl. Nano Mater. 5, 605-614.
515 Stavitskaya, A.V., Kozlova, E.A., Kurenkova, A.Y., Glotov, A.P., Selischev, D.S., Ivanov, E.V., Kozlov, D.V.,
516 Vinokurov, V.A., Fakhrullin, R.F., Lvov, Y.M., 2020. Ru/CdS Quantum Dots Templated on Clay Nanotubes as
517 Visible-Light-Active Photocatalysts: Optimization of S/Cd Ratio and Ru Content. Chemistry – A European
518 Journal 26, 13085-13092.
519 Ulakpa, W.C., Ulakpa, R.O.E., Eyankware, E.O., Egwunyenga, M.C., 2022. Statistical optimization of biodiesel
520 synthesis from waste cooking oil using NaOH/ bentonite impregnated catalyst. Cleaner Waste Systems 3,
521 100049.
522 Viseras, C., Viseras, C.I., López-Galindo, A., 2000. Characteristics of Pharmaceutical Grade Phyllosilicate
523 Powders. Pharmaceutical Development and Technology 5, 47-52.
524 Wan, Z., Lim, J.K., Hameed, B.H., 2017. Chromium–tungsten–manganese oxides for synthesis of fatty acid
525 methyl ester via esterification of palm fatty acid distillate. Energy 141, 1989-1997.
526 Wang, X., Li, C., Lam, C.H., Subramanian, K., Qin, Z.-H., Mou, J.-H., Jin, M., Chopra, S.S., Singh, V., Ok, Y.S., Yan,
527 J., Li, H.-Y., Lin, C.S.K., 2022. Emerging waste valorisation techniques to moderate the hazardous impacts, and
528 their path towards sustainability. J. Hazard. Mater. 423, 127023.
529 Zhang, J., Zhou, C.H., Petit, S., Zhang, H., 2019. Hectorite: Synthesis, modification, assembly and applications.
530 Appl. Clay Sci. 177, 114-138.
531 Zhang, Q., Lei, Y., Li, L., Lei, J., Hu, M., Deng, T., Zhang, Y., Ma, P., 2023. Construction of the novel PMA@Bi-
532 MOF catalyst for effective fatty acid esterification. Sustainable Chemistry and Pharmacy 33, 101038.
533 Zhang, Q., Yang, T., Lei, D., Wang, J., Zhang, Y., 2020. Efficient Production of Biodiesel from Esterification of
534 Lauric Acid Catalyzed by Ammonium and Silver Co-Doped Phosphotungstic Acid Embedded in a Zirconium
535 Metal-Organic Framework Nanocomposite. ACS Omega 5, 12760-12767.
536 Zhang, W., Li, M., Wang, J., Zhao, Y., Zhou, S., Xing, W., 2017. Heterogeneous poly(ionic liquids) catalyst on
537 nanofiber-like palygorskite supports for biodiesel production. Appl. Clay Sci. 146, 167-175.
538 Zhou, C.H., Keeling, J., 2013. Fundamental and applied research on clay minerals: From climate and
539 environment to nanotechnology. Appl. Clay Sci. 74, 3-9.

540

541